Cable Force Analysis of Gi-Lu Cable-Stayed Bridge after Gi-Gi Earthquake

Z.K. Lee[1], K.C. Chang[2], C.H. Loh[2], C.C. Chen[3] and C.C. Chou[4]

[1)] Associated researcher of National Center for Research on Earthquake Engineering, Taipei, Taiwan
[2)] Professor of National Taiwan University, Taipei, Taiwan
[3)] Associated Professor of Yunlin University of Science and Technology, Yunlin, Taiwan
[4)] Graduate student of National Taiwan University, Taipei, Taiwan

Abstract

Located at Nantou Country, Gi-Lu Bridge is a modern designed pre-stressed concrete cable-stayed bridge, which crosses the longest river (Juosheui River) in Taiwan. With two 120-meter spans and harped sixty-eight cables, the bridge is supported by a single pylon and two bents at the ends of the spans. On September 21, 1999, near upon the constructional completion of Gi-Lu Bridge, a significant earthquake (Gi-Gi Earthquake) with 7.3 M_L magnitude seriously struck the central part of Taiwan. For only three kilometers away from the epicenter, the bridge underwent very strong ground shaking and its several structure members broke: one cable fell onto the deck, the protective layer of the pylon peeled off, the cap beams of the two side-span bents were ruined by the pounding force of the deck and the bents, and between the anchors and anchor seats, steel plates bent seriously: it was believed that the cable forces had redistributed. After the main shock, the emergency repair work was implemented immediately, and most of the repair work was finished by July, 2001. However, more different than expected, the recondition work of the cable-system is still put off up to now. To prepare the future repair work of the cable system, the owner, Directorate General of Highways, entrusted the cable system investigation to National Center for Research on Earthquake Engineering (NCREE). The above-mentioned is the subject for this paper. From the view point of structure engineering, Gi-Gi Earthquake had serious damaged the bridge and the cable forces had redistributed; therefore, the identification of the present cable forces is the primary and fundamental study. In this paper, using the in-suit experiment data, the authors will quantify the mechanical property of the cable-system. At the end of this paper, according to analysis result, several engineering suggestions concerning the cables' recondition project will be proposed.

INTRODUCTION

Located at Nantou Country, Gi-Lu Bridge is a modern designed pre-stressed concrete cable-stayed bridge, which crosses the longest river (Juosheui River) in Taiwan. As shown in Fig.1 and Fig.2, the bridge has a single pylon (58 meters height above the deck), two rows of harped cables (68 cables in total), and a streamline-shape single box girder. With 2.75 meters in depth and 24 meters in width, the box girder rigidly connects with the pylon and spans 120 meters to each side span. On September

21, 1999, near upon the constructional completion of Gi-Lu Bridge, a significant earthquake (Gi-Gi Earthquake) with 7.3 M_L magnitude seriously struck the central part of Taiwan. For only three kilometers away from the epicenter, Gi-Lu Bridge underwent very strong ground shaking and several of its structure members broke: one cable fell onto the deck, the concrete cover of the pylon peeled off, the cap beams of the two bents were ruined by the pounding force of the deck and the bents, the girder near the pylon buckled, and several steel plates between the anchors and anchor seats bent seriously: it was believed that the cable forces had redistributed. Gi-Lu Bridge became the first earthquake damaged cable-stayed bridge in the world.

After the main shock, the emergency repair was implemented immediately to support the bridge for the following aftershocks' striking, and all the mending of the concrete structure had been finished by July, 2001. Nevertheless, the repair of the cable system is still put off up to now because the status of this bridge is unknown and the ways to repair the cable system is not clear. In order to partly relieve the pressure of local traffic demand for small cars and to prepare the future repair work, the owner Directorate General of Highways entrusted National Center for Research on Earthquake Engineering (NCREE) in July 2002 with an in-suit loading test and the investigation of the cable-system and the bridge. The above-mentioned is the subject of this paper. From the view point of structural engineering, Gi-Gi Earthquake had serious damaged the bridge and the cable forces had redistributed; therefore, the identification of the present cable forces is the primary and fundamental study. In the following article, using the in-suit experiment data, the authors will quantify the mechanical property of the cable-system, and at the end of this paper, according to analysis result, several suggestions concerning the cables' recondition project will be proposed.

CONTENT OF THIS PAPER

The purpose of this paper is to more precisely identify the status of all cables and the bridge itself. Compared with String Vibration Theory, the dynamic behavior of a real cable system is much more complex: many physical factors are not considered in String Theory, such as gravity, moment inertia, rubber damping effect, boundary condition and temperature effect. To roughly describe the difference between String Theory and a real cable system, the following equation can be used:

$$\text{Real cable force} \approx \text{String Theory estimation} - \text{gravity effect} - \text{moment inertia effect} - \text{boundary condition effect} - \text{damping rubber effect} \ (\pm \text{temperature effect consideration}) \quad (1)$$

Equation (1) indicates that the force estimation by String Theory ($T=4\times w\times f_1 l^2/g$) tends to be greater than the true force since those factors increase the fundamental frequency of a cable. The above-mentioned qualitatively describes the difference between String Theory and a real system. In the following article, "inverse-problem" techniques will be adopted to more precisely analyze the cable forces. For concise demonstration, a shortest cable, a longest cable and a middle-length cable will be considered, and for comparison, the identified cable forces will be compared with the result by practical formulas [1]. Finally at the end of this paper, the whole cables will be globally examined and suggestion together with a bridge model concerning re-prestressing the cables will be proposed.

BASIC DATA AND YOUNG'S MODULUS ANALYSIS OF THE CABLES

Basic Datum of the Cables

As shown in Table 1, all basic data about the cables are listed. Table 1(a) is the cables' labels with

relative positions; Table 1(b) is the number of wire cords in each cable; Table 1(c) the density the cables; Table 1(d) the designed length; Table 1(e) the angle of elevation; Table 1(f) the designed cable force at the third construction stage (final stage).

Young's modulus Analysis of the Cables

Young's modulus is one of the most fundamental parameters concerning materials' behavior. To make sure the Young's modulus of the cables is primarily important for analyzing the cable forces; therefore, some experiment on the cable is implemented. In the girder, the authors hit anchors by wooden rods to generate longitudinal wave, and velocimeters are attached to the cables to measure the longitudinal vibration. Then according to spectrum analysis and theory of wave propagation in rods, the Young's modulus of the cables can be calculated by the following equation:

$$V = \sqrt{\frac{E}{r}} = 2 \times L \times f_1 \qquad (2)$$

where V is the speed of wave propagation, L is the length of cable, f_1 is the first dominant frequency. For Cable R33, the calculated Young's modulus is 1.87E11 N/m^2; and 1.83E11 N/m^2 for both Cable R25 and Cable R17. In the following article, 1.87E11 N/m^2 is adopted for the analysis of all sixty-eight cables.

SYSTEM IDENTIFICATION ON ONE OF THE SHORTEST CABLES

In this section, by signal spectrum analysis and FEM analysis, the transverse vibration signal (on gravity plane) are applied to identify the cable force, sectional moment inertia and boundary condition of Cable L1. The signal spectrum of Cable L1 is shown in Fig.3 and two major features are observed: firstly the intervals between two sequential dominant frequencies gradually increase with the order number; secondly a smaller peak is located around 4.8Hz (this small peak is caused by the vibration of the pylon). Concerning the former, String Theory must not satisfy the experiment result since the dominant frequencies in the theory group as an algebraic series which is derived from the following equation:

$$T = \frac{4w}{n^2 g}(f_n l)^2 \qquad (3)$$

where $\boldsymbol{T}$ is the cable force, $\boldsymbol{g}$ is the gravity acceleration，$\boldsymbol{n}$ is the order number of dominant frequency，f_n is the nth dominant frequency. With no doubt, the moment inertia of the cable helps with the increasing intervals of the dominant frequencies. However, once the moment inertia is involved, what kind of boundary condition is suitable for the real system? Hinges, fixed ends, or hinges with rotational springs? In summary, the cable force, the moment inertia and the boundary condition all need to be analyzed.

Influence of Boundary Condition

As the above-mentioned, String Theory can not simultaneously agree with the five observed frequencies on Fig.3 It's possible to fit those frequencies if a beam model is adopted to simulate Cable L1. Assume the gravity effect can be neglected for the shortest cables; a beam model for Cable L1 is created according to its density and designed length on Table 1(c) and Table 1(d). Two ideal boundary conditions are considered: hinges and fixed ends. Then the study becomes an optimization problem searching for the "best" cable force parameter and moment inertia parameter so that the created model can satisfy the observed, unequal-spaced dominant frequencies. Table 2 lists two parameter sets for the two ideal boundary conditions. To surprise, the two models both satisfy the experiment, but there is 14% difference in the cable force. This means that the 14% cable force

can't be determined solely from the vibration signal, and the 14% cable force relates with the boundary condition of the anchor system.

Consider the following conjecture. Given a hinge with a rotational spring at each end of L1 cable, no matter what the stiffness is, there exists an optimized parameter set which satisfies the observed unequal-spaced dominant frequencies. In other words, both the cable force and the moment inertia are function of the stiffness of the rotational spring. Fig.4 illustrates such a relationship; both hinge end and fixed end are two extreme cases, and the real anchor system could be any point on the line. In the next section, the equivalent stiffness of the rotational spring for the anchor system will be studied, and the cable force will be determined.

Anchor System Analysis

In this section the anchor system will be analyzed by FEM, and a curve regarding the anchor's equivalent rotational stiffness under various axial forces will be established. Then such this curve will be incorporated into Fig.4 to determine the cable force of Cable L1.

Fig.5 shows the anchor system FEM model: Fig.5 (a) about the anchor, the anchor seat and the boundary, Fig.5 (b) about the mesh, and Fig.5 (c) about the structure relationship between each component. Both the anchor and anchor seat are measured in-suit, and the material properties of concrete and steel plates are assumed to be those in the designed blueprint. The components contact with each other, and the friction coefficient is assumed to be 0.2; therefore the equivalent rotational stiffness is function of the axial force (cable force) applied on the anchor. Two steps are used in the analysis: (1) Apply certain axial force on the anchor. (2) Give a disturbance moment on the anchor and calculate the equivalent rotational stiffness according to the following expression:

$$K_q = \frac{\Delta M}{\Delta q} \qquad (4)$$

Fig.6 draws the curve about equivalent rotational stiffness under various cable forces. Finally, both Fig.4 and Fig.6 incorporated into Fig.7, two curves intersect and yield the cable force: 3.07E6 N, just a little bit larger than the fixed-end case. Another phenomenon is concerned and predicted: the longer the cable length is, the smaller the $\Delta T/T$ ratio on Fig.7 shall become. Based on the above analysis, in the following cases, all the boundary conditions are assumed to be fixed ends for convenience.

SYSTEM IDENTIFICATION ON ONE OF THE LONGEST CABLES

By comparing signal spectrum with the characteristic frequencies in FEM model, the cable force, the moment inertia, and the sag of Cable R34 will be identified in this section.

Fig.8 shows the signal spectrum of Cable R34 and lists twenty-three dominant frequencies. About this figure, two major features are observed: (1) Double f_1 is lager than f_2. (2) The intervals between two sequential dominant gradually increase with the order number of dominant frequencies. The latter feature can be explained by moment inertia; however, the former feature is contributed by gravity effect. In the following analysis, a model considering "gravity effect," "geometry nonlinearity," and "moment inertia" will be analyzed and optimized to satisfy the observed twenty-three dominant frequencies on Fig.8.

All the basic data about Cable R34 are listed on Table 1. For convenience, some known physical parameters are described as follows: (1) Angle of elevation 26^o. (2) Designed length 126.42 m. (3)

Length density 47.9kg/m. (4) Young's modulus 1.83E11 N/m^2. (5) Cross section area 0.0060 m^2. (6) Gravity 9.81m/sec^2. In the analytical model, the whole structure is subjected to gravity and fixed-end boundary conditions, and the cable is composed of one thousand beam elements.

Having established the analytical model, the remaining task is searching the "best" solution of the cable force and the moment inertia so that the optimized model agrees with the observed twenty-three dominant frequencies. Through the optimization process, the identified cable force is 1.66E6 N, and the identified moment inertia is 5.0E-6 m^4. The configuration of Cable R34 is shown in Fig.9; the sag at the middle is 49 cm, and the cable force is only 91.4% (1.66E6 N/ 1.81E6 N) of the force estimated by String Theory. Table 3 lists the dominant frequencies in both the experimental result and the analytical result. Good agreement is achieved.

SYSTEM IDENTIFICATION ON ONE OF THE MIDDLE-LENGTH CABLES

By comparing signal spectrum with the characteristic frequencies in FEM model, the cable force, the moment inertia and the sag of Cable R17 will be identified in this section.

Fig.10 shows the signal spectrum of Cable R17 and lists twelve dominant frequencies. About this figure, two major features are observed: (1) Double f_1 is almost equal to f_2. (2) The intervals between two sequential dominant frequencies gradually increase with the order number ($f_3 - f_2 = 1.7325$ Hz、$f_7 - f_6 = 1.7781$ Hz 、$f_{11} – f_{10} = 1.8865$ Hz). Still, the second feature can be explained by moment inertia, while the former feature suggests that this system is close to String Theory. In the following analysis, a model considering "gravity effect," "geometry nonlinearity," and "moment inertia" will be analyzed and optimized to satisfy the observed twelve dominant frequencies on Fig.10.

All the basic data about Cable R17 are also listed on Table 1. For convenience, some known physical parameters are described as follows: (1) Angle of elevation 31^o. (2) Designed length 76.41 m. (3) Length density 47.9Kg/m. (4) Young's modulus 1.83E11 N/m^2. (5) Cross section area 0.0060 m^2. (6) Gravity 9.81m/sec^2. In the analytical model, the whole structure is subjected to gravity and fixed-end boundary conditions, and the cable is composed of one thousand beam elements.

Having established the analytical model, the remaining task is searching the "best" solution of the cable force and the moment inertia so that the optimized model agrees with the observed twelve dominant frequencies. Through the optimization process, the identified cable force is 3.26E6 N, and the identified moment inertia is 5.0E-6 m4. The configuration of Cable R17 is shown in Fig.11; the sag at the middle is 8.8 cm, and the cable force is 97% (3.26E6 N/3.36E6 N) of the force estimated by String Theory. Table 4 lists the dominant frequencies in both the experimental result and the analytical result. Good agreement is achieved.

COMPARISON WITH THOSE FORCES CALCULATED BY PRACTICAL FORMULA

In 1996, Hiroshi Zui, Tohru Shinke and Yoshio Namita proposed a set of formulas for the calculation of cable forces [1]. Under the assumption of fixed-end boundary conditions, they derived a set of practical formulas in the aim that field engineers can quickly and directly calculate cable forces. What an engineer need is the signal spectrum, ***cable sag***, angle of elevation, and some fundamental data, such as Young's modulus, ***moment inertia***, cross section area, and density. However, it is not an easy task to measure the sags of all cables. In addition, cables are composed of wire cords, and

how to calculate the equivalent moment inertia under different cable forces is a problem. However, based on the previous study in this paper, both the sags and equivalent moment inertia have been identified in the three cases; therefore, the practical formula is applicable to check the FEM results. The formulas are shortly described as follows:

if $3 \le \Gamma$

$$T = \frac{4w}{g}(f_1 l)^2[1 - 2.20\frac{c}{f_1} - 0.550(\frac{c}{f_1})^2] \qquad 17 \le x \qquad (5)$$

$$T = \frac{4w}{g}(f_1 l)^2[0.865 - 11.6(\frac{c}{f_1})^2] \qquad 6 \le x \le 17 \qquad (6)$$

$$T = \frac{4w}{g}(f_1 l)^2[0.828 - 10.5(\frac{c}{f_1})^2] \qquad 0 \le x \le 6 \qquad (7)$$

if $\Gamma \le 3$

$$T = \frac{w}{g}(f_2 l)^2[1 - 4.40\frac{c}{f_2} - 1.10(\frac{c}{f_2})^2] \qquad 60 \le x \qquad (8)$$

$$T = \frac{w}{g}(f_2 l)^2[1.03 - 6.33\frac{c}{f_2} - 1.58(\frac{c}{f_2})^2] \qquad 17 \le x \le 60 \qquad (9)$$

$$T = \frac{w}{g}(f_2 l)^2[0.882 - 85.0(\frac{c}{f_2})^2] \qquad 0 \le x \le 17 \qquad (10)$$

where

$$c = \sqrt{\frac{EIg}{wl^4}} \quad x = \sqrt{\frac{T}{EI}}l \quad \Gamma = \sqrt{\frac{wl}{128EAd^3\cos^5 q}}(\frac{0.31x + 0.5}{0.31x - 0.5})$$

, and some symbols are defined in Fig.12.

Verification on Cable L1

A=0.00756m^2， E=1.83e11N/m^2， I=17.55E-6 m^4，
g=9.8 m/sec^2， l=29.3 m ， f_1=4.12 Hz
θ=55/360×2×π，ρ=61.2 kg/m ， w=ρg。

Calculate the c parameter：

$$c = \sqrt{\frac{EIg}{wl^4}} = 0.2673$$

Apply Equation(5)：

T= 3.05E6 N

Check ξ：

ξ = 28.5061 (O.K.)

Verification on Cable R34

A=0.0060m^2， E=1.83E11N/m^2， I=5.0E-6 m^4，
g=9.8 m/sec^2，l=126.4 m，f_1=0.769 Hz、f_2=1.499 Hz
θ=26/360×2×π， ρ=47.8 kg/m ， w=ρg，
l_o=l×cosθ ， s=0.49 m ， δ=s/l_o。

Calculate the c parameter：

$$c = \sqrt{\frac{EIg}{wl^4}} = 0.0087$$

Apply Equation(8)：

T= 1.6723E6 N

Check ξ and Γ：

ξ = 170.6 Γ=2.5939<3 (O.K.)

Verification on Cable R17

$A=0.0060m^2$ ， $E=1.83E11N/m^2$ ， $I=4.57E\text{-}6\ m^4$ ，
$g=9.8\ m/sec^2$ ， $l=76.4\ m$ ， $f_1=1.732\ Hz$ ，
$\theta=31/360\times2\times\pi$ ， $\rho=47.8\ kg/m$ ， $w=\rho g$ ，
$lo=l\times\cos\theta$ ， $s=0.088\ m$ ， $\delta=s/lo$ 。

Calculate the *c* parameter：

$$c=\sqrt{\frac{EIg}{wl^4}}=0.0227$$

Apply Equation(5)：

T= 3.25E6 N

Check ξ and Γ：

ξ = 150.7　　3<Γ=12.2　　(O.K.)

The cable forces from the above calculation are almost identical to those by the FEM optimization analysis. This means that, at least, the results by the practical formulas are consistent with the results by the identification procedure in this paper. In addition, it's unnecessary to measure the sag and to get the moment inertia of a cable in advance when the identification procedure is applied.

DISCUSSION ON THE PRESENT CABLE SYSTEM AND SUGGESTIONS ON THE REPAIR PROJECT

By the identification technique, all the 68 cables are identified. Table 5 lists the identified cable forces, the designed cable forces, and the ratio of difference. Two features are observed from Table 5. Firstly, those cable forces around the Cable L14 are obviously greater than the designed. Secondly, those cable forces near the two side spans are much lower than the designed. Therefore the cable forces around the middle spans, in general average, are larger than the designed. From the above observation, it is suggested that Cable L14 should be set up first in the repair project. Then it is recommended to strengthen those cable forces near the two side spans. The purpose of these suggestions is to gain a better balance status for the replacement of other cables. Besides, for practically monitoring the cable force in each cable during the repair engineering, this study has built up a series of figures (such as Fig.13) which draw the relationship between the cable forces and the fundamental frequencies, dot the present status of each cable, and mark ± 10% region centering around the designed force. Finally, as shown in Fig.14, a bridge model incorporating all the present cable forces and the present deck elevation has been built up. This bridge model, together with the above-mentioned figures, is intended to aid the repair project.

REFERENCES

[1] Hiroshi Zui, Tohru Shinke, and Yoshio Namita, "Practical Formula for Estimation of Cable Tension by Vibration Method," Journal of Structural Engineering, June 1996, p651~656.

[2] Design Drawings for the Gi-Lu Cable-stayed Bridge, T.Y. Lin International, 1995.

[3] "ABAQUS USER MANUAL," Hibbitt, Karlsson, and Sorensen, Inc.

[4] Charles Chadwell, Near-Source Earthquake on the Ji-Lu Cable-stayed Bridge in the 21 September 1999 Chi-Chi Taiwan Earthquake," Phd. Dissertation, Berkeley, 2001.

Table 1(a)：Label of Cables　Table 1(b)：Number of wire cords　Table 1(c)：Density
Table 1(d)：Designed Length　Table 1(e)：Angle of Elevation　Table 1(f)：Designed Cable Force

Table 1(a)

Gi-Gi	
33	33
31	31
29	29
27	27
25	25
23	23
21	21
19	19
17	17
15	15
13	13
11	11
9	9
7	7
5	5
3	3
1	1
#	Label
2	2
4	4
6	6
8	8
10	10
12	12
14	14
16	16
18	18
20	20
22	22
24	24
26	26
28	28
30	30
32	32
34	34
Lu-Ku	

Table 1(b)

Gi-Gi	
43	43
55	55
55	55
55	55
43	43
55	55
43	43
43	43
43	43
43	43
43	43
43	43
37	37
37	37
43	43
43	43
55	55
number of wire cords	
55	55
43	43
43	43
37	37
37	37
43	43
43	43
43	43
43	43
43	43
43	43
43	43
55	55
43	43
55	55
55	55
55	55
43	43
Lu-Ku	

Table 1(c)

Gi-Gi	
0.480	0.480
0.613	0.613
0.613	0.613
0.613	0.613
0.480	0.480
0.610	0.610
0.480	0.480
0.480	0.480
0.480	0.480
0.480	0.480
0.480	0.480
0.480	0.480
0.412	0.412
0.412	0.412
0.480	0.480
0.480	0.480
0.613	0.613
Density	kg/cm
0.613	0.613
0.480	0.480
0.480	0.480
0.410	0.410
0.410	0.410
0.480	0.480
0.480	0.480
0.480	0.480
0.480	0.480
0.480	0.480
0.480	0.480
0.480	0.480
0.610	0.610
0.480	0.480
0.613	0.613
0.613	0.613
0.613	0.613
0.480	0.480
Lu-Ku	

Table 1(d)

Gi-Gi	
12642.2	12642.2
12006.3	12006.3
11381.8	11381.8
10757.4	10757.4
10125.6	10125.6
9508.9	9508.9
8879.4	8879.4
8258.0	8258.0
7640.5	7640.5
7024.8	7024.8
6412.0	6412.0
5804.1	5804.1
5201.1	5201.1
4608.1	4608.1
4028.1	4028.1
3465.7	3465.7
2980.3	2980.3
Designed length : cm	
2980.3	2980.3
3465.7	3465.7
4028.1	4028.1
4608.1	4608.1
5201.1	5201.1
5804.1	5804.1
6412.0	6412.0
7024.8	7024.8
7640.5	7640.5
8256.0	8256.0
8879.4	8879.4
9508.9	9508.9
10125.6	10125.6
10757.4	10757.4
11381.8	11381.8
12006.3	12006.3
12642.2	12642.2
Lu-Ku	

Table 1(e)

Gi-Gi	
26.0	26.0
27.0	27.0
27.0	27.0
27.0	27.0
27.0	27.0
28.0	28.0
29.0	29.0
30.0	30.0
31.0	31.0
33.0	33.0
34.0	34.0
36.0	36.0
38.0	38.0
41.0	41.0
45.0	45.0
49.0	49.0
55.5	55.5
Angle of elevation:°	
55.5	55.5
49.0	49.0
45.0	45.0
41.0	41.0
38.0	38.0
36.0	36.0
34.0	34.0
33.0	33.0
31.0	31.0
30.0	30.0
29.0	29.0
28.0	28.0
27.0	27.0
27.0	27.0
27.0	27.0
27.0	27.0
26.0	26.0
Lu-Ku	

Table 1(f)

Gi-Gi	
229.8	229.8
270.4	270.4
254.0	254.0
243.1	243.1
233.7	233.7
227.5	227.5
231.6	231.6
220.8	220.8
264.4	264.4
257.2	257.2
255.0	255.0
240.9	240.9
230.8	230.8
227.5	227.5
228.7	228.7
258.6	258.6
288.1	288.1
Designed cable force	
288.1	288.1
258.6	258.6
228.7	228.7
227.5	227.5
230.8	230.8
240.9	240.9
255.0	255.0
257.2	257.2
264.4	264.4
220.8	220.8
231.6	231.6
227.5	227.5
233.7	233.7
243.1	243.1
254.0	254.0
270.4	270.4
229.8	229.8
Lu-Ku	

Table 2: Optimized Parameters for the Two Ideal Boundary Conditions

	Measured dominant frequencies: Hz	String Theory	Analytical characteristic frequencies: Hz (fixed-end)	Analytical characteristic frequencies: Hz (hingy-end)
f_1	**4.12**	**4.12***	**4.14**	**4.13**
f_2	**8.43**	**8.24***	**8.43**	**8.41**
f_3	**12.97**	**12.36***	**12.99**	**12.96**
f_4	**17.93**	**16.48***	**17.94**	**17.91**
f_5	**23.26**	**20.60***	**23.38**	**23.35**
Moment inertia		0. m⁴	1.95E-5 m⁴	1.74E-5 m⁴
Cable force		3.5786 N	3.57E6 N±0.09	3.57E6 N±0.83

$2f_1 < f_2$

* an algebraic series

Table 3 : Dominant frequency Comparison between the Experiment and Analysis for R34 Cable

	Experiment	Analysis
Mode No.	Hz	Hz
1	0.769	0.769
2	1.499	1.496
3	2.248	2.247
4	2.997	2.999
5	3.751	3.755
6	4.511	4.514
7	5.279	5.278
8	6.044	6.047
9	6.833	6.822
10	7.591	7.604
11	8.386	8.393
12	9.176	9.19
13	9.978	9.996
14	10.802	10.81
15	11.631	11.63
16	12.455	12.47
17	13.303	13.32
18	14.167	14.18
19	15.021	15.05
20	15.907	15.93
21	16.821	16.83
22	17.733	17.74
23	18.635	18.67

Table 4 : Dominant frequency Comparison between the Experiment and Analysis for R17 Cable

	Experiment	Analysis
Mode No.	Hz	Hz
1	1.7327	1.7325
2	3.4628	3.4629
3	5.1953	5.2001
4	6.9496	6.9435
5	8.7043	8.696
6	10.476	10.459
7	12.2541	12.236
8	14.0303	14.028
9	15.8487	15.837
10	17.6494	17.665
11	19.5359	19.515
12	21.3985	21.387

Table 5: Identified Cable forces, Designed Cable Forces, and Ratio of Difference

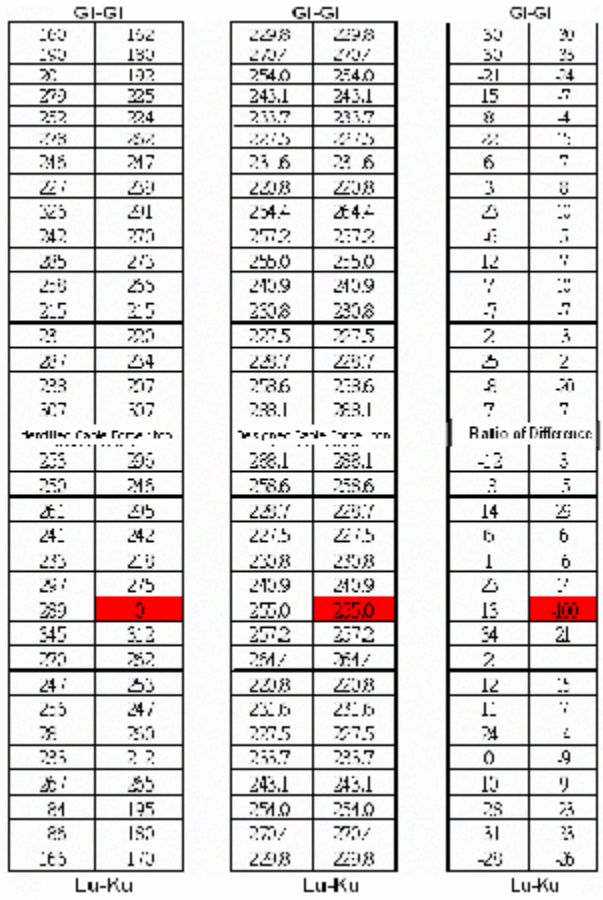

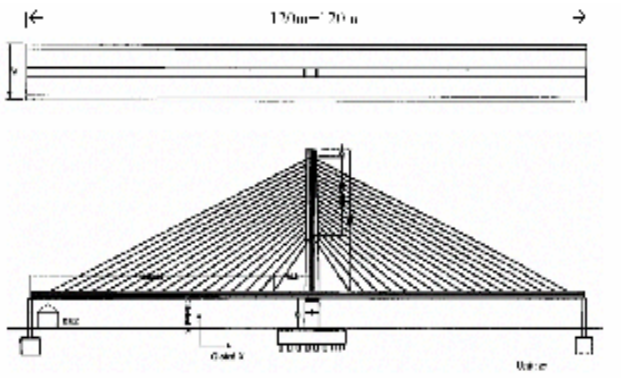

Fig. 1: Top View and Side View of Gi-Lu Cable-Stayed Bridge

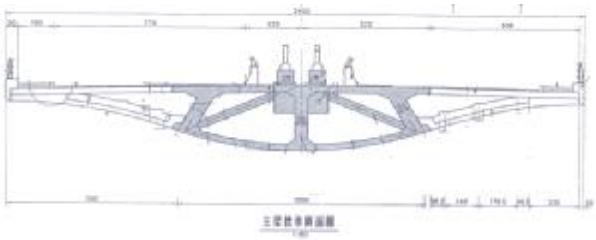

Fig. 2: Cross Section of the Box Girder

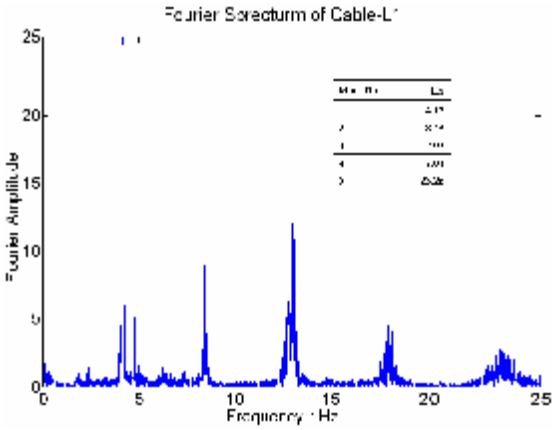

Fig. 3: Spectrum Analysis of Cable L1

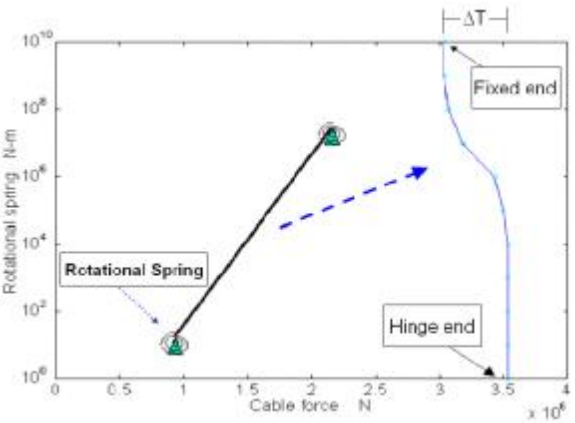

Fig. 4: Relationship between the Moment Inertia and the Cable Force of Cable L1

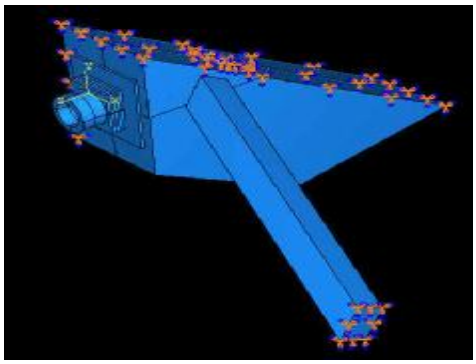

Fig. 5(a): Anchor, Anchor Seat and Boundary

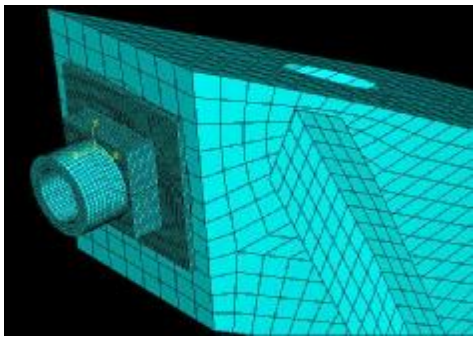

Fig. 5(b): The Mesh

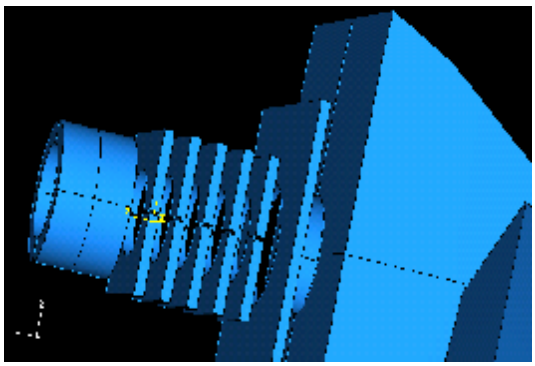

Fig. 5(c): Assembly of Each Component

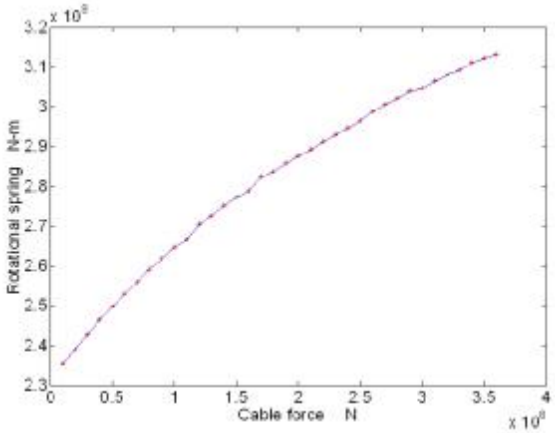

Fig. 6: Equivalent Rotational Spring under Different Cable Force

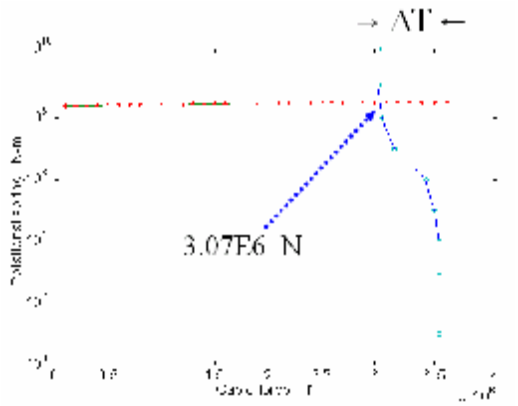

Fig. 7: Incorporation both Fig. 4 & Fig. 6, and the Cable-Force Solving of Cable L1

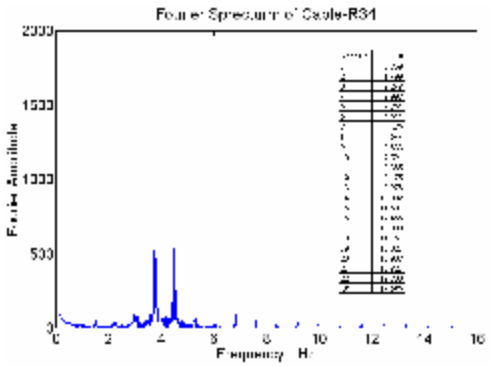

Fig. 8: Signal Spectrum of Cable R34 and the Twenty-Three Dominant Frequencies

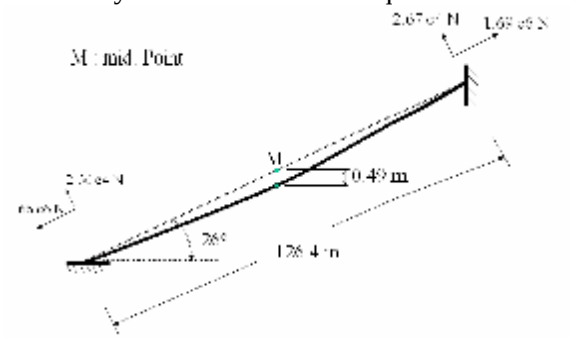

Fig. 9: Identified Configuration of Cable R34

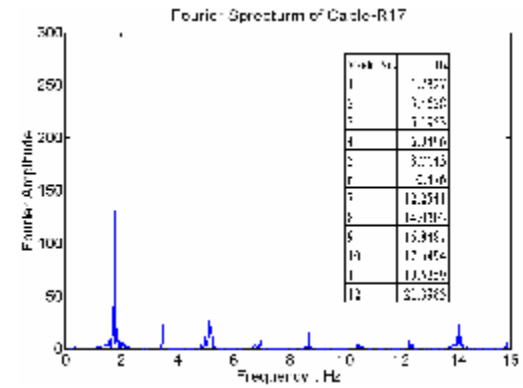

Fig. 10: Signal Spectrum of Cable R17 and the Twelve Dominant Frequencies

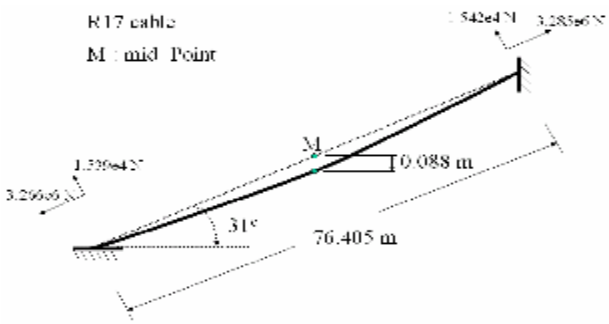

Fig. 11: Identified Configuration of Cable R17

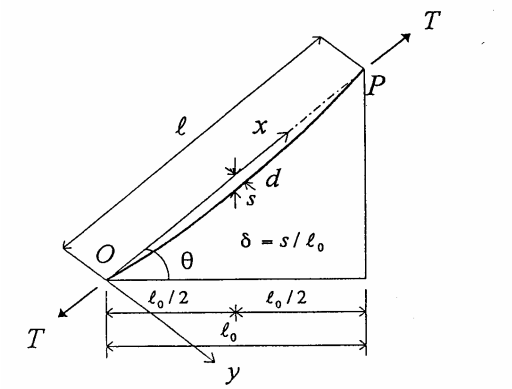

Fig. 12: Symbol Definition of a Cable

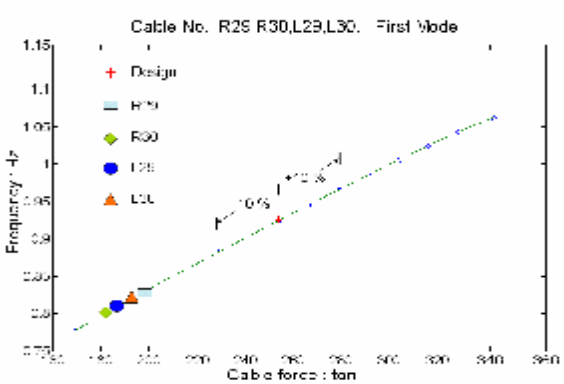

Fig. 13: Present Status and the Relationship Curve between the Cable Forces vs. the Fundamental Frequencies of Cable R29, R30, L29, L30

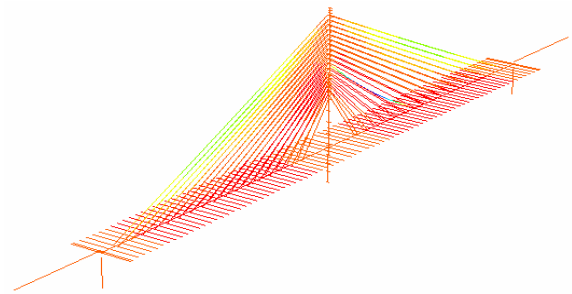

Fig. 14: Gi-Lu Bridge Model Intended to Aid the Repair Project (Incorporating all the Present Cable Forces and Deck Elevation)